DOI: 10.1002/chem.200701119

DFT Modeling of Silver Disorder and Mobility in the Semiconductor Cluster $[Ag_{28}S_{26}(P(O)PhOMe)_{12}(PPh_3)_{12}]$

Nathan R. M. Crawford,[a] Claudia Schrodt,[a] Alexander Rothenberger,[b, c] Weifeng Shi,[b] and Reinhart Ahlrichs*[a]

Abstract: Disorder of silver atoms and high cation mobility are commonly observed and closely coupled features in silver chalcogenides. The ligand-stabilized cluster $[Ag_{28}(\mu_6\text{-}S)_2\{ArP(O)S_2\}_{12}(PPh_3)_{12}]$ (**1**) (Ar = 4-anisyl), with a total of 666 atoms, displays in its X-ray structure highly localized disorder at two core silver atoms. To explore the nature of this disorder, we have applied density functional methods to its internal structure and flexibility. The pseudo-S_6 symmetry of the cluster provides six equivalent pockets to place the pair of silver atoms, and with the exception of populating neighboring sites, all permutations relax to structures with similar cores. The barrier to concerted motion of the central silver atoms from one set of pockets to the next of the C_i-symmetric conformer is estimated to be less than about 26 kJ mol^{-1}. Cluster **1** can be considered a model for bulk phase cation mobility.

Keywords: clusters · crystallographic disorder · density functional calculations · molecular dynamics · semiconductors · silver sulfide

Introduction

Bulk silver chalcogenide materials, such as crystalline solids, glasses, and liquids, commonly act as electrical conductors, with the Ag^+ ion as the primary charge carrier.[1–6] While investigating possible molecular precursors to these materials, the cluster compound $[Ag_{28}S_{26}(P(O)PhOMe)_{12}(PPh_3)_{12}]$ (**1**, Scheme 1 and Figure 1) was synthesized. The data extracted from the X-ray diffraction (XRD) study on the crystal were insufficient to fully characterize the state of the cluster in the solid. While the exterior of the cluster was very well defined, the organic ligands showed some conformational disorder, and the central core of the cluster had significant disorder.[7] Electron density representing two silver atoms was distributed over six sites corresponding to three pairs of C_i-related atom positions with apparent percentage occupation weights of 60:20:20 (Figure 2, right). Additionally, two pairs of silver atoms further from the core were each split into two positions separated by 50 pm. A third pair of silver atoms was not visibly split, but was related to the former pairs by a pseudo-threefold rotation. Interestingly, except for the two disordered silver atoms at its core and some conformational disorder of phenyl groups, the molecule has S_6 symmetry, although only the inversion center is strictly enforced by the crystal symmetry.

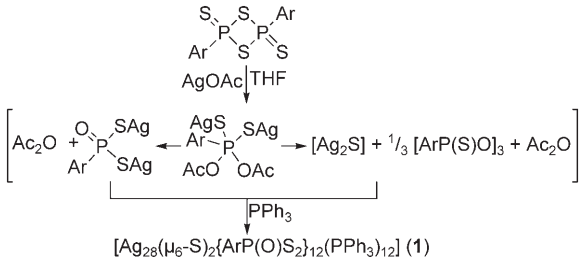

Scheme 1. Synthesis of **1** (Ar = 4-anisyl).

These observations lead to questions. Was the silver disorder due to the entire cluster settling into various orientations during crystallization, or were the central silver atoms

[a] N. R. M. Crawford, C. Schrodt, Prof. Dr. R. Ahlrichs
Institut für Physikalische Chemie
Kaiserstrasse 12, 76131 Karlsruhe (Germany)
E-mail: reinhart.ahlrichs@chemie.uni-karlsruhe.de

[b] Dr. A. Rothenberger, W. Shi
Institut für Anorganische Chemie
Kaiserstrasse 12, 76131 Karlsruhe (Germany)

[c] Dr. A. Rothenberger
Institut für Nanotechnologie, Forschungszentrum Karlsruhe
Postfach 3640, 76021 Karlsruhe (Germany)

Supporting information for this article is available on the WWW under http://www.chemeurj.org/ or from the author. It includes 11 optimized conformations of **1** and their truncated average; optimized *ortho*, *meta*, and *para* conformers of **1**; and three oxidation states of **2** in *xyz* format.

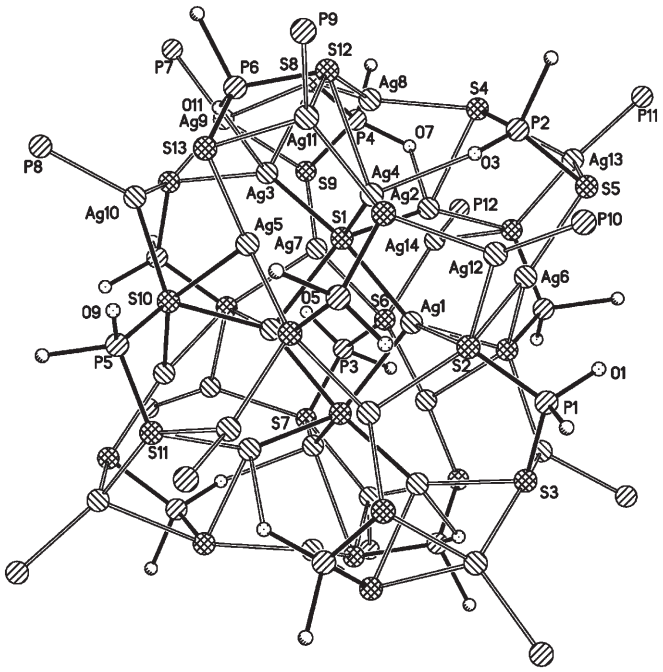

Figure 1. Molecular structure of **1** in the solid state (disordered components and phenyl groups were omitted; only α-C atoms of 4-anisyl- substituents are displayed). Selected ranges of bond lengths [Å]: Ag–S 2.212(3)–2.925(2), Ag–P 2.4077(19)–2.4153(16), Ag–O 2.426(5)–2.503(4), P–S 2.037(3)–2.087(2), P–O 1.489(4)–1.506(4), Ag···Ag 2.7632(3)–3.3670(18).

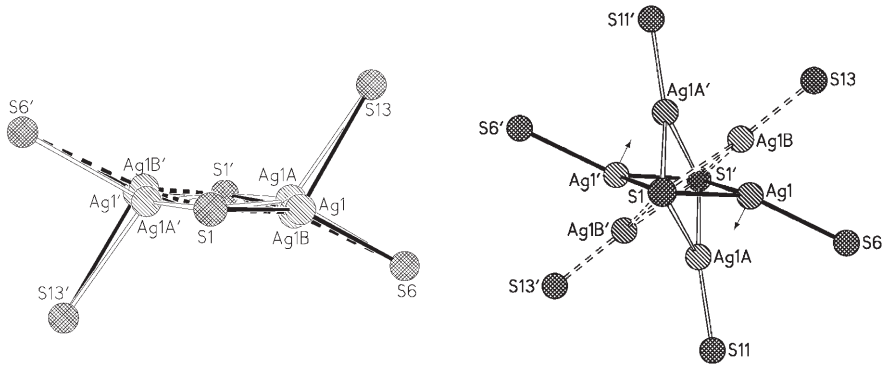

Figure 2. Disorder in the core of **1**. Representation of the central Ag_2S_2 unit, which is slightly disordered in the new crystal (left), but heavily disordered in the previously published result (right, ref. [7]). Arrows in the image on the right represent the initial velocity vectors of the central silver atoms in the molecular dynamics trajectory.

actively jumping among the six symmetry-related local environments, similar to the conduction of Ag^+ in the bulk? How tightly coupled are conformational changes of the ligands and the interior of the cluster, and does one determine the other? Is there enough room in the core to support a third silver (in line with the threefold nature of the rest of the cluster), but with its additional electron density being masked by the X-ray refinement artificially contracting the nearby inorganic shell?

To answer these questions, XRD of new crystals of **1** were performed, and extensive molecular electronic structure calculations conducted. With this study, we continue our recent successful characterization of problematic inorganic structures by the combined use of quantum chemical methods and XRD.[8–10] We apply density functional theory to check the quality of putative structures by comparing computed energies and optimized geometries with those from the X-ray investigation, giving a more definitive picture of the molecule. We next describe the details of experiment and computation, their results, and derive from them conclusions about the nature of the compound.

Experimental and Computational Details

Crystals of **1** were prepared according to a published procedure[7] and remeasured. Details of the original structure determination can be obtained free of charge The Cambridge Crystallographic Data Centre (CCDC-283239) via www.ccdc.cam.ac.uk/data_request/cif. Data were measured on a STOE IPDS II diffractometer by using $Mo_{K\alpha}$ radiation. The structures were solved by direct methods, and refined by full-matrix least-squares against F^2 using all data (see Table 1 for details).[11] Hydrogen atoms were placed in idealized positions.

The TURBOMOLE v5.8 quantum chemistry software package was used for all electronic structure calculations. Unless otherwise noted, all calculations were conducted with the DFT functional BP86[12] using the def-SV(P) (split-valence plus polarization functions on the non-hydrogen atoms) orbital and auxiliary basis sets[13] plus corresponding 28-electron effective core potential[14] on silver. Integration was performed on the m3 multilevel quadrature, and checked in part on m4.[13c] Interelectronic Coulomb interaction was treated with the resolution of the identity (RI-*J*) method[15] together with the multipole-accelerated resolution of the identity approximation (MARI-*J*).[16] Geometric structures were optimized by a relaxation procedure based on analytic gradients[13b] of the energy and using redundant internal coordinates;[17] geometries were considered converged when the differences in energies between consecutive iterations were below 5×10^{-5} E_h and the norm of the gradient dropped below 4×10^{-3} in atomic units.

A very limited ab initio molecular dynamics calculation was carried out solely for estimating the barrier to concerted motion of a pair of silver atoms from one pocket to the next. For this, the same functional and basis sets as in the geometry optimizations were used. To save CPU time, an SCF energy convergence criterion of 10^{-5} E_h was employed instead of the usual 10^{-6} E_h. The leapfrog algorithm to propagate molecular geometry based on the DFT gradients was used. It was considered sufficient to use a relatively large time step of 80 atomic time units (1.935 fs). Additionally, the high-frequency C–H bond vibrations were damped by using a minor modification of the SHAKE[18] and RATTLE[19] algorithms that conserve translational and angular momentum of the constrained atoms, while the constrained bond lengths were allowed to vary by up to 0.01 Bohr per time step to adjust to conformational changes in the ligands. The total system energy was monitored to give a measure of integration error.

Table 1. X-ray data collection parameters for two crystals of **1**·2 Et_2O·2 THF.

Compound	**1** (ref. [7]; CCDC: 283239)	**1** (this work)
formula	$C_{300}H_{264}Ag_{28}O_{24}P_{24}S_{26}$·2 Et_2O·2 THF	$C_{300}H_{264}Ag_{28}O_{24}P_{24}S_{26}$·2 Et_2O·2 THF
formula weight	9935.90	9935.90
T/K	100	100
crystal system	triclinic	triclinic
space group	$P\bar{1}$	$P\bar{1}$
a [Å]	22.8410(6)	22.824(1)
b [Å]	23.4102(7)	23.347(1)
c [Å]	23.8337(6)	23.891(1)
α [°]	118.290(2)	117.683(3)
β [°]	96.031(2)	97.838(3)
γ [°]	113.295(2)	112.942(4)
V [Å^3]	9609.6(5)	9563.1(8)
Z	1	1
μ [mm^{-1}]	1.692	1.700
F(000)	4952	4952
reflections collected	77691	48366
unique data	39248	32620
R_{int}	0.0458	0.0418
parameters	1943	1943
wR_2 (all data)	0.1945	0.1781
R_1 [$I > 2\sigma(I)$]	0.0630	0.0547

Results and Discussion

X-ray structural analysis: The diffraction data of the title compound were originally modeled as a neutral cluster on an inversion center, with two central silver atoms disordered over six sites. The charge was based on the lack of counterions detected in the crystal structure, as well as the crystallization from THF not easily supporting the small counterions (H^+, OH^-) that might go unnoticed among disordered solvent molecules. The disorder of the central silver atoms is the main roadblock in determining the exact nature of this cluster, and is exacerbated by the large number of refinement parameters available. The Ag_2S_2 core of the X-ray structure is a distorted rhombus with the S(1)···S(1′) diagonal tilted slightly from the pseudo-threefold axis, and the major equatorial silver atom positions at 60% occupancy. Two additional inversion-related pairs of Ag at 20% occupancy are related to the first by rough S_6 operations about the pseudo-axis. It is not immediately clear if the disorder is primarily temporal or translational, or if a possible third silver atom could be comfortably accommodated.

To get a qualitative picture of the disorder present in **1**, the X-ray structure determination of **1** was repeated on several newly grown crystals. A comparison of the new and old datasets indicates that a significant decrease in disorder of the central Ag atom Ag(1) (Figure 2) was possible, probably due to small changes in crystallization conditions. The bulk of the cluster, including even the conformationally disordered phenyl ligands, remained almost unchanged despite a change in the disorder of central silver atoms, suggesting a very low energy barrier to central silver rearrangement. The likely fluxional nature of the cluster supports the hypothesis that **1** could be considered as a model compound for solid silver-based ion conductors, and initiated a comprehensive DFT study.

DFT analysis of disorder in 1: As a first step, we examined the structure suggested by the previously published X-ray refinement. Eleven starting geometries for **1** were generated by populating various C_i-symmetry combinations of disordered silver sites; two more initial structures were generated by populating two central silver positions separated by 60° ("*ortho*") or 120° ("*meta*") rotation about the core S···S axis. All structures featured the complete ligand shell, and were relaxed to local minimum-energy geometries while maintaining initial symmetry.

All C_i starting geometries converged to essentially identical structures, which could be mapped onto each other by rotational symmetry operations of the S_6 prototype. Truncating the computed structures at phosphorus, the inorganic portions were overlaid to minimize the mass-weighted difference in the positions of corresponding atoms, which were then averaged to generate the structure $\mathbf{1}_{av}$. The root-mean-square of absolute differences in the atomic positions of any of these C_i-symmetry computed geometries to those in $\mathbf{1}_{av}$ ranged from 9.3 to 26.6 pm. A similar comparison of $\mathbf{1}_{av}$ to the XRD structures gave an rms difference of 29.5 pm for the old, and 36.3 pm for the new. This means that the deviation of any one computed structure from the average over ligand conformations is of the same magnitude as the deviation of the crystal structure from that same average. Considering that small differences in bond lengths and angles in such a large cluster can add up to large absolute changes at the exterior, this deviation, as can be seen in Figure 3, is indeed very small. As they are directly attached to the ambiguous silver positions, the distance between the axial sulfur atoms should be most susceptible to changing silver

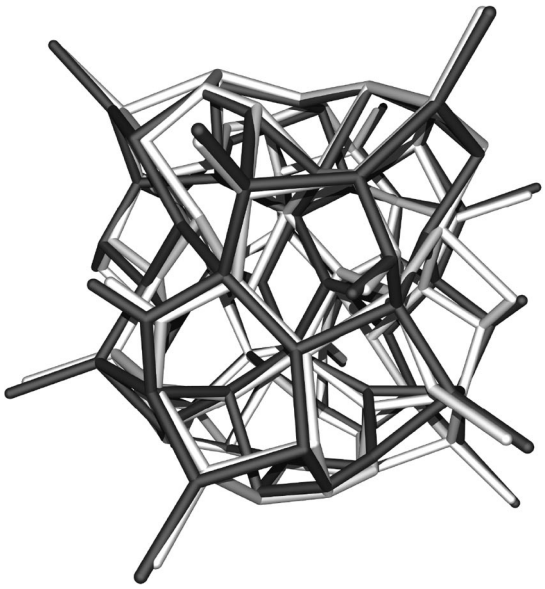

Figure 3. Overlaid interiors of **1** from the new X-ray structure (light) and the average of eleven calculated geometries $\mathbf{1}_{av}$ (dark).

occupancy. The core S(1)···S(1′) distance for the averaged computed structure [394 pm] is close to the experimental distance [398–410 pm].

After discussion of specific structural aspects, we now turn to the examination of bond lengths within the inorganic portion of the cluster, since these are of most direct interest and are usually well reproduced by electronic structure calculations. In Table 2, the averages of two types of Ag–S bond lengths for the new X-ray structure are given with the standard deviation within each group. Although they have essentially identical average distances, the silver atoms that are only bonded to sulfur, largely located in the interior, have double the variation in Ag–S distances as the phosphorous-bonded silver atoms on the exterior. This is likely due to the much more varied local environment of the interior perturbing the Ag–S interaction from its preferred distance.

Table 2. Distance comparison of selected bonds and bond types[a] in pm.

Bond type	X-ray (new)	Δ X-ray (ref. [7])	Δ $\mathbf{1}_{av}$	Δ $\mathbf{1}^{*}$ [b]	Δ $\mathbf{2}^{+}$ [c]
(S)Ag–S[×24]	258.2±9.8	−2.9±3.9	1.8±5.8	3.9±5.5	2.0±7.3
(P)Ag–S[×12]	258.1±5.0	−0.2±1.2	4.2±3.5	3.3±2.8	4.1±3.6

Bond	X-ray (new)[d]	X-ray (ref. [7])[d]	$\mathbf{1}_{av}$	$\mathbf{1}^{*}$ [b]	$\mathbf{2}^{+}$ [c]
Ag(1)–S(1)	248.7–273.7	268.7–276.4	259.4	260.8	268.2
Ag(1)–S(1′)	248.2–252.4	247.3–252.4	259.0	262.9	265.2
S(1)···S(1′)	409.5	398.2	393.9	396.7	377.9
Ag(1)···Ag(1′)	281.5–331.1	329.0–348.7	336.9	341.8	376.4

[a] Bond type differences (Δ) compare each individual bond of a type to its partner in the new X-ray. [b] Computed structure with the worst overlap to $\mathbf{1}_{av}$. [c] The central Ag_3 ring was converted to Ag_2 for comparison by taking the atom that is closest to the X-ray Ag(1) position and generating its inversion image with respect to the center of mass. [d] Measurements including disordered positions are given as a range.

The bond lengths in the new X-ray structure were taken as individual references for comparison with the old structure, as well as with the computed structures. Each of the 24 symmetry-unique interior Ag–S bonds of the old structure was around 3 pm shorter (±4 pm) than its corresponding new version, while the 12 symmetry-unique surface Ag–S bonds were virtually unchanged. It is dangerous to infer too much from such small changes, but this hints that the effects of increasing disorder of the core are isolated from the exterior. The bond lengths in the core are also nearly identical to those of the average computed structure, $\mathbf{1}_{av}$, which are only 2±6 pm longer than those in the reference. This difference in bond lengths is doubled for the exterior Ag–S bonds, but this is attributable to the nearby ligands being exposed to vacuum in the calculations, but a condensed environment in the crystal. The optimized structure of **1** with the most deviance from the average, denoted **1***, was also quite close in bond length statistics.

Our findings imply that independent of the start geometry, structure optimization converges to one of the three pockets where the central silver pair are in *para* positions. This is in line with approximate S_6 symmetry, although without corresponding rotation of the ligand shell, thereby indicating that the cluster core is largely decoupled from ligand conformation changes. There are, however, consequences to ligand conformation changes: seven of the optimized structures have energies within 30 kJ mol^{-1} of the lowest, while one is higher by 92 kJ mol^{-1}.

A natural population analysis (NPA)[20] was conducted to elucidate the degree of ionicity within the cluster. Results are in agreement with chemical intuition, with charges on silver varying between +0.52 and +0.67, and most sulfur between −0.71 and −0.76, with the exception of the central sulfur pair at −1.11 each. The variation reflects the number and electronegativity of surrounding atoms, with the large negative charge at the central sulfur atoms being in line with an environment of five silver atoms.

The observed disorder of the central silver atoms as a rough hexagon may also be the result of occasional breaking of C_i symmetry: going from an Ag-S-S-Ag torsion angle of 180° to a torsion of ≈120° or ≈60°. Geometry optimizations starting from these "*meta*" and "*ortho*" configurations proceeded rapidly to the observed pseudo-C_i "*para*" structure, but to eliminate them as possibilities a more rigorous approach was required. Three geometry optimizations, starting from a C_3-symmetric conformation of the ligands, were carried out with the central Ag-S-S-Ag torsion angle constrained to 60°, 120°, or 180°. As anticipated, the *ortho* conformer relaxes to a significantly distorted geometry that is 50 kJ mol^{-1} higher than the *para*. Surprisingly, the *meta* conformer relaxes to a geometry that, apart form the constrained silvers, is almost indistinguishable from the *para*, only an insignificant 4 kJ mol^{-1} higher in energy, and consistent with the X-ray structure anaylsis. This is clearly not enough to eliminate the *meta* conformer as a significant contributor to the ensemble and likely source of the lower-occupancy silver positions.

DFT analysis of $[Ag_{29}S_{26}(P(O)PhOMe)_{12}(PPh_3)_{12}]$, 2: The geometries of the +1, 0, and −1 charge states of **2**, an analogue of the structure solved by X-ray diffraction in which a third silver atom was added to the core to form an Ag_3 triangle, were optimized under C_3 symmetry. The cores of the calculated Ag_{29} clusters form trigonal bipyramids with sulfur atoms at the axial positions and a triangle of silver atoms on the equator. The positively and negatively charged clusters had closed-shell electronic configurations with HOMO–LUMO gaps of 1.46 eV and 0.72 eV, respectively. The neutral molecule was closer to the anion in both geometric and electronic structure, with a singly occupied *a*-type HOMO, analogous to the HOMO of the anion. The calculated S···S distance in the positive cluster [378 pm] is shorter than the experimentally detetrmined distances of 398–410 pm, while those in the neutral [432 pm] and negative [448 pm] are too long. When truncated to the ligand phosphorus atoms, and retaining only one of the core silver atoms (and its inversion image), the computed cluster geometry can be superimposed on that of the crystal to give rms absolute deviations

of 36.86, 38.83, and 41.92 pm for the positive, neutral, and negative clusters respectively. The Ag_3 versions of the cluster are not unreasonable, but do not match the X-ray data nearly as well as the Ag_2, and are therefore quite unlikely.

Barrier estimation of Ag_2 motion in 1: To estimate barriers to central silver motion, a highly restricted molecular dynamics simulation on the full neutral Ag_{28} cluster was performed by using the same density functional and basis set as the geometry optimizations. A full exploration of the ab initio potential energy surface, required for a thorough kinetic description of the transition, is clearly not feasible for us at present, since one time step takes around four hours. A single trajectory was thus generated from a fully relaxed C_i-symmetric molecule at 0 K and adding 93 kJ mol^{-1} of kinetic energy (each) to the two central silver atoms. The velocities of Ag(1) and Ag(1′) (Figure 2) were in the direction of Ag(1A) and Ag(1A′) respectively. Their inversion-related velocity vectors (6×10^{-4} atomic units) were nearly in the equatorial plane and tangential to a circle about the pseudo-S_6 axis. The C_i-symmetry initial conditions allowed the simulation to run completely under C_i symmetry, saving computational resources and simplifying interpretation.

As can be seen in Figure 4, the first maximum in the potential energy is reached at 78 fs. This is slightly over

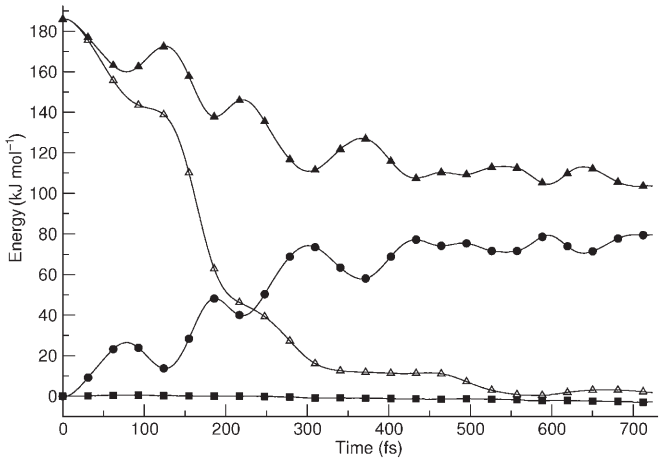

Figure 4. Energy distribution during the molecular dynamics trajectory of **1**, as started from the configuration and velocities in Figure 2. The lines with circles and filled triangles respectively represent relative potential and kinetic energy of the system. Open triangles follow the kinetic energy of the two central silver atoms. Deviation from total energy conservation is shown with squares.

26 kJ mol^{-1} above the local minimum, representing an upper bound for the barrier to concerted motion of the central silver pair from one S_6 pocket to the next. As this small value is on par with the possible uncertainty due to the method of computation, the most we can say is that this barrier is relatively small. The second potential energy minimum of the trajectory at 126 fs is close to a local minimum of the structure, and converges to that in a standard geometry optimization. A third, shallow, dip in potential energy is found 221 fs along the trajectory, and relaxes to a local minimum corresponding to another of the S_6 pockets.

Conclusion

Starting from the X-ray structures, several C_i symmetry arrangements of the disordered silver positions were subjected to structure optimization, which all resulted in geometries with inorganic cores that could be overlaid with pseudo-S_6 rotations. The ligand conformations of all starting geometries were identical, and did not change appreciably on relaxation, resulting in different relative conformations of ligand to core. It is clear from this that conformational changes in the ligands should not significantly affect the core. Populating the central silver positions in a *meta* arrangement leads to a similar energy, while the *ortho* geometry can be excluded. If either *para* or *meta* arrangements were statistically distributed over the pockets, they would be consistent with the observed C_i symmetry X-ray result. Furthermore, the barrier for the concerted 120° rotation of the *para* silver dimer from one well to another is no more than about 26 kJ mol^{-1}, indicating that a fluxional nature of the cluster is allowed even at low temperatures.

The theoretical treatment described in this work answers several questions that arose from the initial disordered crystal structure. The X-ray results, as they measure an ensemble of conformations, are fully consistent with both the dynamic and static (or combination thereof) disorder models. Although theoretically reasonable, the cluster with a central Ag_3 unit contains too much electron density at the core to be compatible with experiment. Compound **1** is not particularly large for a semiconductor cluster, yet it is able to support large changes in the internal geometry and even the total number of silver cations without distortion of the exterior. It is quite possible that similarly pliant local geometries account for the cation conduction in silver chalcogenides.

Acknowledgements

This work has been supported by the DFG Center for Functional Nanostructures, and the Fonds der Chemischen Industrie. We also thank Christopher E. Anson for helpful discussions regarding crystallographic disorder.

[1] C. J. Benmore, P. S. Salmon, *Phys. Rev. Lett.* **1994**, *73*, 264.
[2] T. Kawaguchi, *J. Non-Cryst. Solids* **2004**, *345*, 265.
[3] M. N. Kozicki, M. Mitkova, *J. Non-Cryst. Solids* **2006**, *352*, 567.
[4] M. Ribes, E. Bychkov, A. Pradel, *J. Optoelectron. Adv. Mater.* **2001**, *3*, 665.
[5] F. Salam, J. C. Giuntini, J. V. Zanchetta, *Ionics* **1995**, *1*, 171.
[6] T. Wagner, *J. Optoelectron. Adv. Mater.* **2002**, *4*, 717.
[7] W. Shi, R. Ahlrichs, C. E. Anson, A. Rothenberger, C. Schrodt, M. Shafaei-Fallah, *Chem. Commun.* **2005**, 5893.
[8] R. Ahlrichs, C. E. Anson, D. Fenske, O. Hampe, A. Rothenberger, M. Sierka, *Angew. Chem.* **2003**, *115*, 4169; *Angew. Chem. Int. Ed.* **2003**, *42*, 4036.

[9] R. Ahlrichs, D. Fenske, M. McPartlin, A. Rothenberger, C. Schrodt, S. Wieber, *Angew. Chem.* **2005**, *117*, 4002; *Angew. Chem. Int. Ed.* **2005**, *44*, 3932.
[10] R. Ahlrichs, D. Fenske, A. Rothenberger, C. Schrodt, S. Wieber, *Eur. J. Inorg. Chem.* **2006**, 1127.
[11] G. M. Sheldrick, SHELX-97, Program for the Solution of Crystal Structures, Universität Göttingen, **1997**.
[12] S. Vosko, L. Wilk, M. Nussair, *Can. J. Phys.* **1980**, *58*, 1200. A. D. Becke, *Phys. Rev. A* **1988**, *38*, 3098. J. P. Perdew, *Phys. Rev. B* **1986**, *33*, 8822.
[13] a) A. Schäfer, H. Horn, R. Ahlrichs, *J. Chem. Phys.* **1992**, *97*, 2571; b) K. Eichkorn, O. Treutler, H. Öhm, M. Häser, R. Ahlrichs, *Chem. Phys. Lett.* **1995**, *242*, 652; c) K. Eichkorn, F. Weigend, O. Treutler, R. Ahlrichs, *Theor. Chem. Acc.* **1997**, *97*, 119.
[14] D. Andrae, U. Haeussermann, M. Dolg, H. Stoll, H. Preuss, *Theor. Chim. Acta* **1990**, *77*, 123.
[15] K. Eichkorn, O. Treutler, H. Öhm, M. Häser, R. Ahlrichs, *Chem. Phys. Lett.* **1995**, *240*, 283.
[16] M. Sierka, A. Hogekamp, R. Ahlrichs, *J. Chem. Phys.* **2003**, *118*, 9136.
[17] M. von Arnim, R. Ahlrichs, *J. Chem. Phys.* **1999**, *111*, 9183.
[18] J. P. Ryckaert, G. Ciccotti, H. J. C. Berendsen, *J. Comput. Phys.* **1977**, *23*, 327.
[19] H. C. Andersen, *J. Comput. Phys.* **1983**, *52*, 23.
[20] A. E. Reed, R. B. Weinstock, F. Weinhold, *J. Chem. Phys.* **1985**, *83*, 735.

Received: July 20, 2007
Published online: November 7, 2007

